Enhancement of dopamine sensing by layer-by-layer assembly of PVI–dmeOs and Nafion on carbon nanotubes

2010 Nanotechnology 21 215601

(http://iopscience.iop.org/0957-4484/21/21/215601)

Nanotechnology **21** (2010) 215601 (8pp) doi:10.1088/0957-4484/21/21/215601

Enhancement of dopamine sensing by layer-by-layer assembly of PVI–dmeOs and Nafion on carbon nanotubes

Hui-Fang Cui[1,3], Yu-Han Cui[1], Yu-Long Sun[1], Kuan Zhang[1] and Wei-De Zhang[2]

[1] Department of Bioengineering, Zhengzhou University, 100# Science Avenue, Zhengzhou 450001, People's Republic of China
[2] School of Chemistry and Chemical Engineering, South China University of Technology, Guangzhou 510641, People's Republic of China

E-mail: hfcui@zzu.edu.cn

Received 14 December 2009, in final form 19 March 2010
Published 30 April 2010
Online at stacks.iop.org/Nano/21/215601

Abstract

In this study, carbon nanotubes (CNTs) were modified to further improve their performance in electrochemical sensing of dopamine (DA) levels. After a redox polymer, poly(vinylimidazole) complexed with Os(4,4′-dimethyl-2,2-bipyridine)$_2$Cl (termed PVI–dmeOs) was electrodeposited on multi-wall CNTs (MWCNTs), Nafion and PVI–dmeOs films were successfully layer-by-layer (LBL) assembled on the hydrophilic surface of the as-prepared PVI–dmeOs/CNTs nanocomposites through electrostatic interactions. The LBL assembly was proved by scanning electron microscopy (SEM), electrochemistry and UV–vis spectroscopy measurements. LBL assembly of Nafion/PVI–dmeOs films on CNTs significantly enhanced their linear sweep voltammetry (LSV) response sensitivity to DA, with a maximum enhancement for three Nafion/PVI–dmeOs film-modified MWCNTs. The LSV peak current density of (Nafion/PVI-dmeOs)$_3$/CNT electrodes in response to 10 and 50 μM DA solutions was about 7.3 and 3.9 times those for bare CNTs. At the (Nafion/PVI-dmeOs)$_3$/CNT electrodes, the limit of detection (LOD) (signal-to-noise ratio: 3) was 0.05 μM DA, the linear range was 0.1–10 μM DA (with a linear regression coefficient of 0.97) and the DA-sensing sensitivity was 8.15 μA cm^{-2} μM^{-1}. The newly fabricated (Nafion/PVI-dmeOs)$_3$/CNT electrodes may be developed as an ideal biosensor for direct and *in situ* measurement of DA levels.

(Some figures in this article are in colour only in the electronic version)

1. Introduction

Dopamine (DA) is a prevalent catecholamine neurotransmitter in the brain. Degeneration of dopaminergic neurons, the predominant cause of Parkinson's disease (PD), causes reduced DA concentrations, even DA depletion, in the striatum and probably in other basal ganglia areas [1]. DA is electrochemically active (oxidizable), allowing the employment of electrochemical techniques in the detection of DA levels. Electrochemical detection is a simple, sensitive and environmentally friendly detection method that is even suitable for the analysis of colored or turbid samples. However, the electrochemical detection of DA in physiological samples is quite challenging due to the coexistence of high ascorbic acid (AA) levels (0.2–0.5 mM) with the low level of DA (10^{-8}–10^{-7} M) in physiological samples [2, 3], where DA is positively charged, while AA is negatively charged. AA is not only an electrochemically active (oxidizable) compound but also electrochemically oxidized at a very close potential to that of DA at conventional unmodified electrodes [4, 5].

The discovery of carbon nanotubes (CNTs) in 1991 by Iijima [6] offered an excellent novel electrode material for DA sensing. Consisting of cylindrical graphene sheets with nanometer diameters, CNTs, both single-wall and multi-wall CNTs (SWCNTs and MWCNTs, respectively), have high electrical conductivity, high chemical stability and extremely

[3] Author to whom any correspondence should be addressed.

high mechanical strength [7, 8]. The subtle electronic properties of CNTs suggest that CNTs have the ability to promote electron-transfer reactions [9]. Several reports have demonstrated a strong, highly reversible and diffusion-controlled process of electrocatalytic two-electron oxidation of DA at CNT electrodes [9–11]. Loh and his co-workers [12] showed that AA was oxidized at an about 160 mV lower potential than DA at MWCNT electrodes. However, the limit of detection (LOD) still could not satisfy the direct measurement of physiological DA levels. Modification of CNTs could be a solution to further enhance their DA-sensing sensitivity.

On conventional electrodes, various modification strategies have been explored and exploited to enhance DA detection sensitivity and selectivity. Among these strategies, most were coating electrodes with a layer of a negatively charged polymer, such as polyeugenol [13] and Nafion [14–16], to make use of their charge accumulation effect for DA and their charge discrimination effect between AA and DA. Modifying electrodes with electrocatalytic materials, such as CNTs and redox polymers, is another strategy to enhance the detection sensitivity to DA.

Redox polymers are soluble polymers complexed with redox moieties, such as poly(vinylpyridine) (PVP) complexed with $[Os(bpy)_2Cl]^+$ (termed PVP–Os) [17] (bpy: 2,2′-bipyridine) and poly(vinylimidazole) (PVI) complexed with $Os(4,4'\text{-dimethylbpy})_2Cl$ (termed PVI–dmeOs) [18]. When crosslinked on electrodes, the redox polymers become insoluble, but swell in water to form three-dimensional redox hydrogels [19]. Upon swelling, the mobility of their segments increases, increasing the frequency of electron-transferring collisions between the tethered redox centers, and the electronic conductivity of the redox hydrogels. In addition to conducting electrons, the redox hydrogel also conducts ions [20, 21]. Water-soluble species are permeable inside the redox hydrogels. Electroactive water-soluble molecules like nitrite, AA and DA can be electrocatalytically oxidized or reduced in the three-dimensional redox hydrogels [14, 22, 23].

Motivated by taking the advantages of the electrocatalytic activity of redox polymers to DA and the charge discrimination and accumulation effects of negatively charged polymers, Ju *et al* [14] simultaneously covered glassy carbon (GC) electrodes with the PVP–Os redox polymer and Nafion films by droplet evaporation of the corresponding solutions. This dual-film-modified GC electrode exhibited good electrocatalytic activity for DA, by efficiently eliminating the interference from AA. However, the thickness, evenness and porosity of the films cannot be precisely controlled by using this simple dropping and evaporating process. In addition, employment of a conventional GC electrode puts limitations on the performance of this DA sensor.

Recently, we reported the electrodeposition of a thin film of redox polymer PVI–dmeOs on high density vertically aligned MWCNTs [24], which were grown on Ta substrates by the method of chemical vapor deposition [25, 26]. The Ta-supported MWCNTs are easy to be fabricated to form CNT electrodes, and are mechanically robust during detection processes [27, 28]. The electrodeposited PVI–dmeOs molecules are covalently crosslinked on the surface of CNTs and therefore are quite stable during storage and detection processes, changing the surface of CNTs from hydrophobic to hydrophilic [24]. The production of hydrophilic CNTs without impairing their physical properties could expand their applications in many fields, for example, biomaterials, composites and biosensors [29]. In this study, we investigate the layer-by-layer (LBL) assembly of Nafion/PVI–dmeOs films on the hydrophilic PVI–dmeOs/CNT electrodes and the electrocatalytic response of the as-prepared $(\text{Nafion/PVI-dmeOs})_n$/CNT electrodes ($n$ is the number of LBL-assembled Nafion/PVI–dmeOs films) to DA. The thickness of the Nafion/PVI–dmeOs film, and thus the electrochemical performance of the $(\text{Nafion/PVI-dmeOs})_n$/CNT electrodes, should be able to be exactly controlled and reproduced by this LBL assembly process. The overall sensing properties of the $(\text{Nafion/PVI-dmeOs})_n$/CNT electrodes to DA may be optimized by adjusting the number of Nafion/PVI–dmeOs films. The integrated effect of CNTs and LBL-assembled Nafion/PVI–dmeOs films may make this $(\text{Nafion/PVI-dmeOs})_n$/CNT electrode a promisingly ideal DA sensor.

2. Experimental details

2.1. Instrument and reagents

The morphologies of modified MWCNTs were observed by scanning electron microscopy (SEM) (JEOL JSM 6700F, operated at 5 kV). UV–vis spectroscopy measurements were performed using a Beckman Du® 640B UV/vis spectrophotometer (Beckman Coulter, Fullerton, CA, USA). Electrochemical measurements were performed using a BAS100B electrochemical analyzer (Bioanalytical Systems, Inc., IN, USA) in a three-electrode system, including a working electrode (MWCNTs or GC electrode), a platinum counter electrode and a 3 M KCl–Ag|AgCl reference electrode, at room temperature (≈25 °C). All potentials were quoted versus this reference electrode.

Ta plates were obtained from Goodfellow Cambridge Ltd (Huntingdon, UK). All the chemicals were bought from Sigma-Aldrich Co. (Saint Louis, MO, USA) and were used without further purification. Phosphate buffer solution (PBS) contains: 8 g l^{-1} NaCl, 0.2 g l^{-1} KCl, 1.44 g l^{-1} Na_2HPO_4 and 0.24 g l^{-1} KH_2PO_4 with pH 7.4. Deionized water obtained from a Millipore water system was used throughout the experiment.

2.2. Methods

2.2.1. Synthesis of vertically aligned MWCNTs and construction of MWCNT electrodes. MWCNTs were synthesized on small Ta plates (with a size about 3 mm × 3 mm). A very thin layer of cobalt (Co) was deposited on Ta plates by magnetron sputtering to serve as a catalyst for MWCNT growth. The high density vertically aligned MWCNTs were grown on Co-coated Ta plates by chemical vapor deposition with ethylenediamine as a precursor at 880 °C for 5–10 min. The detailed synthetic method and the characterization of the MWCNTs was described

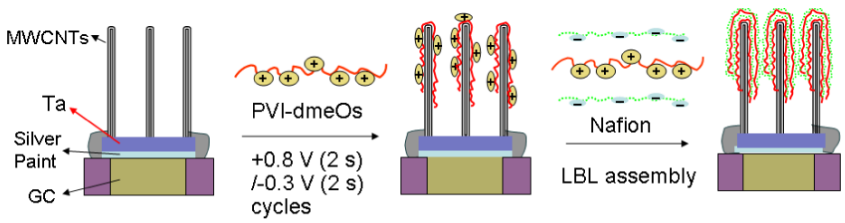

Scheme 1. The schematic construction of MWCNT electrode and the electrodeposition of PVI–dmeOs and LBL assembly of Nafion/PVI–dmeOs films on the MWCNT electrode.

previously [25, 26]. The as-grown MWCNTs have a bamboo-like structure and quite a uniform length and diameter. Their diameters range between 80 and 200 nm, determined by the thickness of the catalyst film, and their lengths are between 5 and 10 μm, depending on the growth time of CNTs. The Ta plate with MWCNTs grown on them was connected to the surface of a GC electrode using conductive silver paint (Structure Probe, Inc., USA). The edge of the Ta plate and GC electrode was insulated by pasting with nail enamel (Maybelline, NY, USA). The as-constructed MWCNT electrodes (schematically shown in scheme 1) were used as working electrodes and for subsequent modification with redox polymer PVI–dmeOs.

2.2.2. Synthesis of redox polymer: poly(vinylimidazole) complexes of [Os(4,4′-dimethylbpy)$_2$Cl] (termed PVI–dmeOs). PVI–dmeOs was synthesized from poly(1-vinylimidazole) (PVI) and Os(4,4′-dimethylbpy)$_2$C1$_2$ by a procedure similar to that of Heller and co-workers [18]. The detailed synthetic procedures for PVI, Os(4,4′-dimethylbpy)$_2$C1$_2$ and PVI–dmeOs were described in a previously published paper [24].

2.2.3. Effective surface area determination of MWCNT electrodes. In order to obtain the effective surface area of the high density vertically aligned MWCNT electrodes, cyclic voltammetry (CV) experiments at bare MWCNTs with $K_3[Fe(CN)_6]$ as a probe were performed. The method to obtain the effective surface area of CNTs was described previously [28]. In this paper, current densities at the MWCNT electrodes with or without modifications were calculated based on the effective surface areas of CNTs.

2.2.4. Electrodeposition of PVI–dmeOs and LBL assembly of (Nafion/PVI-dmeOs)$_n$ films on MWCNT electrodes. A crosslinked film of PVI–dmeOs was irreversibly electrodeposited on an MWCNT electrode from a 1.5 mg ml^{-1} PVI–dmeOs solution supported by PBS. The electrodeposition was achieved by applying repetitive potential step cycles between +0.8 V (2 s) and −0.3 (2 s). The electrodeposition mechanism was described in our published paper [24]. The PVI–dmeOs electrodeposited CNTs electrodes were washed by soaking in a sufficient amount of water for three times. Upon electrodeposition with PVI–dmeOs, the surface of CNTs changed from hydrophobic to hydrophilic, as reported before [24]. The as-prepared PVI–dmeOs/CNTs electrodes were immersed in 2.5% Nafion solution for 3 h, and then rinsed with a sufficient amount of water for three times, producing one Nafion/PVI–dmeOs film on the surface of CNTs (termed (Nafion/PVI-dmeOs)$_1$/CNTs). LBL-assembled multilayer films were grown by alternately immersing the (Nafion/PVI-dmeOs)$_1$/CNT electrodes into 4 mg ml^{-1} PVI–dmeOs solution and 2.5% Nafion solution for 3 h each. A sufficient washing by soaking in water for three times followed after each immersing process. The LBL-assembled film-modified CNTs are referred to as (Nafion/PVI-dmeOs)$_n$/CNTs, where the subscript n represents the number of Nafion/PVI–dmeOs films on the CNT surface. When the outermost layer of the (Nafion/PVI-dmeOs)$_n$/CNT electrode is a PVI–dmeOs film, n will be half an integer, such as 0.5, 1.5, 2.5 and so on. The fabrication of a (Nafion/PVI-dmeOs)$_2$/CNT electrode is schematically illustrated in scheme 1.

2.2.5. Preparation of multilayer films for UV–vis spectroscopy. A quartz slide was cleaned in a bath consisting of three parts 30% H_2O_2 to seven parts concentrated H_2SO_4 at 70 °C. After 30 min, the substrate was removed and washed with water. Immediately after drying the substrate with N_2 gas, it was dipped in a fresh mixture of PVI–dmeOs and poly(ethylene glycol)diglycidyl ether (PEGDGE) (300 μl of 2 mg ml^{-1} PVI-dmeOs + 75 μl of fresh 2.5 mg ml^{-1} PEGDGE). Then the substrate was put into a refrigerator (4 °C) overnight to allow a thin crosslinked PVI–dmeOs film to form on the substrate. Subsequently, Nafion/PVI–dmeOs films were LBL-assembled on the PVI–dmeOs/quartz surface following the same procedure as for PVI–dmeOs/CNTs electrodes. UV–vis spectroscopy measurements were performed on the quartz slide substrate after each Nafion/PVI–dmeOs film was assembled.

2.2.6. Electrochemical characterization of the LBL-assembled (Nafion/PVI-dmeOs)$_n$ films on PVI–dmeOs/CNT electrodes. Following the assembly of Nafion/PVI–dmeOs films on PVI–dmeOs/CNT electrodes, CV experiments of CNTs electrodes in PBS at a scan range between −0.5 and +0.8 V (0.05 V s^{-1}) were performed to characterize the LBL-assembled films. Following each LBL assembly, the redox peaks of a PVI–dmeOs redox hydrogel on CNT electrodes were observed.

2.2.7. Investigation of the DA-sensing sensitivity for LBL-assembled Nafion/PVI–dmeOs film-modified CNT electrodes. The linear sweep voltammetry (LSV) technique was used to detect DA at (Nafion/PVI-dmeOs)$_n$/CNT electrodes in this study. To investigate the effect of the LBL-assembled films on the sensitivity of DA detection, LSVs of 10

and 50 μM DA solutions in PBS at a scan rate of 0.05 V s^{-1} for CNT electrodes modified with different n values of $(Nafion/PVI\text{-}dmeOs)_n$ films were performed. With the optimum n value for DA-sensing sensitivity, LSVs of different concentrations of DA in PBS at the $(Nafion/PVI\text{-}dmeOs)_n$/CNT electrodes were performed.

3. Results and discussion

3.1. Assembly and characterization of $(Nafion/PVI\text{-}dmeOs)_n$ films

The LBL-assembled $(Nafion/PVI\text{-}dmeOs)_n$ films were characterized by using electrochemical, UV–vis and SEM measurements.

3.1.1. Electrochemical characterization of the $(Nafion/PVI\text{-}dmeOs)_n$ films on MWCNT electrodes. Cyclic voltammograms (CVs) of $(Nafion/PVI\text{-}dmeOs)_n$/CNT electrodes with n = 0, 0.5, 1, 1.5 and 2 (curves (a), (b), (c), (d) and (e), respectively) are illustrated in figure 1. As shown in figure 1, a pair of redox peaks with the anodic peak potential (E_{pa}) of +130 mV and the cathodic peak potential (E_{pc}) of +108 mV appear on the CV curve of PVI–dmeOs/CNT electrodes (curve (b)). The redox pairs come from the electro-oxidation and -reduction of the electrodeposited PVI–dmeOs film on the surface of MWCNT electrodes. After soaking in Nafion solution (curve (c)), the E_{pa} and E_{pc} of PVI–dmeOs on the CNTs surface negatively shifted to +110 mV and −4 mV, respectively, resulting in an increase of peak potential difference ($\Delta E_p = E_{pa} - E_{pc}$) from 22 to 114 mV. Accompanying the increase of ΔE_p, the redox peak currents decreased. The decrease of the redox peak currents reflects a decrease of the total amount of redox reactions on the surface of CNTs. The increase of ΔE_p suggests a decrease of the speed of the redox reactions. These results indicate that a Nafion film was formed on the surface of PVI–dmeOs/CNT electrodes. At neutral pH, the imidazol groups of PVI–dmeOs are positively charged, while Nafion is negatively charged. Electrostatic interactions between the positive charges and the negative charges can make a layer of Nafion film be self-assembled on the surface of PVI–dmeOs/CNTs, blocking the electrochemical redox reaction of PVI–dmeOs on the surface of CNT electrodes. A followed soaking in a PVI–dmeOs solution (curve (d)) increased the redox peak current to a level (4.62 μA) that was a little smaller than that of the PVI–dmeOs/CNTs electrode (5.64 μA, curve (b)), but slightly increased the value of ΔE_p to 125 mV (E_{pa}: +121 mV; E_{pc}: −4 mV), suggesting that another PVI–dmeOs film layer was assembled on the surface of the $(Nafion/PVI\text{-}dmeOs)_1$/CNT electrode. This newly assembled PVI–dmeOs film provides more redox groups to the electrode surface, while the membrane resistance of $(Nafion/PVI\text{-}dmeOs)_{1.5}$/CNT electrodes has greatly increased compared with PVI–dmeOs/CNT electrodes, resulting in the increase of ΔE_p.

The increase of membrane resistance with the LBL assembly of Nafion/PVI–dmeOs film was proved by electrochemical impedance spectroscopy (EIS). Figure 2 illustrates

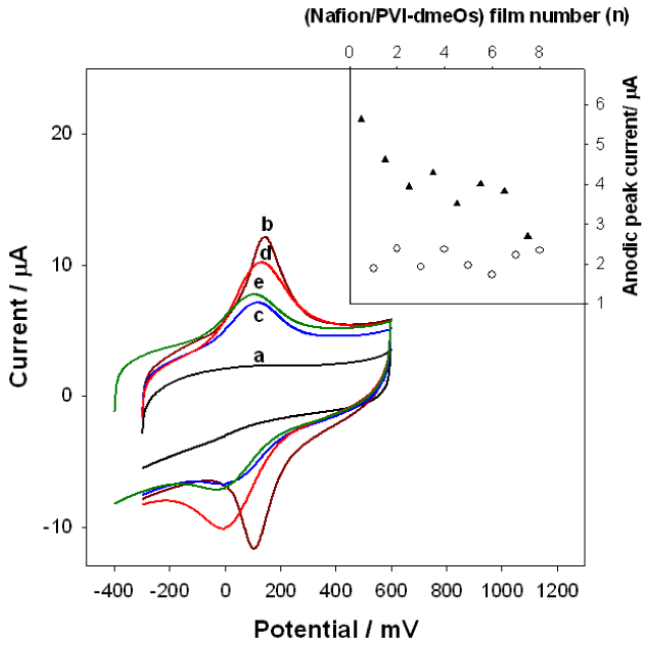

Figure 1. Cyclic voltammograms (CVs) in PBS at a bare MWCNT electrode (a), the CNT electrode electrodeposited with a thin film of PVI–dmeOs (PVI–dmeOs/CNTs) (b) and the PVI–dmeOs/CNTs electrode modified by LBL assembly of a Nafion film $[(Nafion/PVI\text{-}dmeOs)_1/CNTs]$ (c), a subsequent PVI–dmeOs film $[(Nafion/PVI\text{-}dmeOs)_{1.5}/CNTs]$ (d) and then another Nafion film $[(Nafion/PVI\text{-}dmeOs)_2/CNTs]$. Inset: the effect of the number (n) (n = halves: solid triangle; n = integers: hollow circle) of Nafion/PVI–dmeOs films on the anodic peak current of PVI–dmeOs on $(Nafion/PVI\text{-}dmeOs)_n$/CNT electrodes in PBS. Scan rate of CVs: 0.05 V s^{-1}.

the EIS on: (a) MWCNTs, (b) PVI–dmeOs/CNTs and (c) $(Nafion/PVI\text{-}dmeOs)_{1.5}$/CNT electrode in PBS solution containing equimolar $Fe(CN)_6^{3-/4-}$ (10/10 mM) with AC frequency from 0.1 Hz to 100 kHz. Apparent differences in the impedance spectra are observed with these three electrodes. The Nyquist complex plane plot of the bare MWCNT electrode exhibits an almost straight line that is characteristic of a diffusion-limiting step of the electrochemical process. On the other hand, the plot of PVI–dmeOs/CNTs is characterized by a very small single semicircle at high frequency domain and a straight line at low frequency domain. In contrast, the plot of $(Nafion/PVI\text{-}dmeOs)_{1.5}$/CNTs displays a major part of a large semicircle at the high frequency domain and a short head of a straight line at the low frequency domain. The membrane resistance (R_m) of $(Nafion/PVI\text{-}dmeOs)_{1.5}$/CNTs, which can be determined from the semicircle diameter in the Nyquist complex plane plot to be 1436 Ω, is much larger than the R_m of PVI–dmeOs/CNTs (about 18 Ω).

The anodic peak currents of the $(Nafion/PVI\text{-}dmeOs)_n$/CNT electrodes with '$n$' = halves (solid triangle) and 'n' = integers (hollow circle) are illustrated in the inset in figure 1. The anodic peak currents of $(Nafion/PVI\text{-}dmeOs)_n$/CNTs with '$n$' = integers were all around the value of 2.1 μA, while those with 'n' = halves gradually decreased from 5.6 to 2.7 μA (with n from 0.5 to 7.5). The almost stable redox peak currents of $(Nafion/PVI\text{-}dmeOs)_n$/CNT electrodes with '$n$' = integers

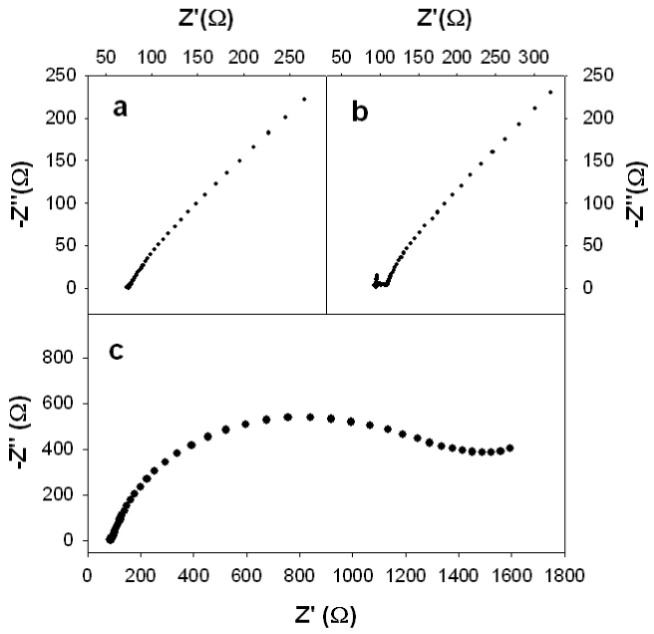

Figure 2. Impedance spectra of (a) MWCNTs, (b) PVI–dmeOs/CNTs and (c) $(\text{Nafion/PVI-dmeOs})_{1.5}$/CNT electrode in PBS solution containing equimolar $Fe(CN)_6^{3-/4-}$ (10/10 mM).

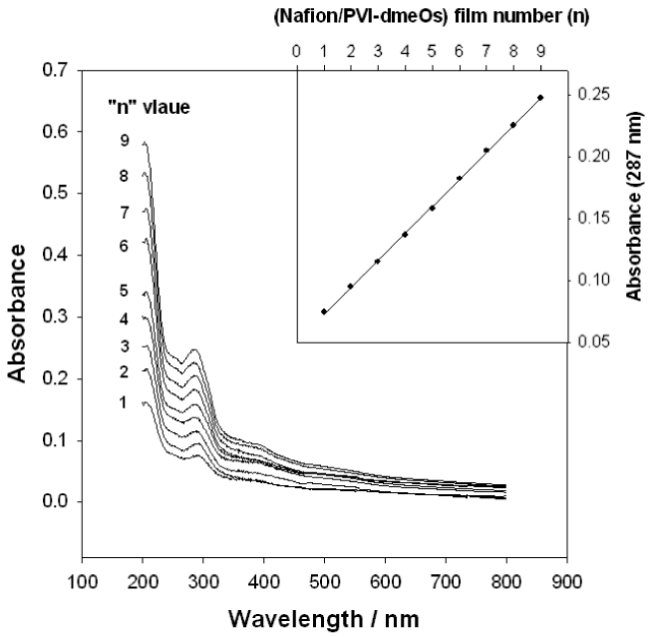

Figure 3. UV–vis absorption spectra of LBL-assembled $(\text{Nafion/PVI-dmeOs})_n$ films on quartz. Inset: the absorbance at 287 nm of the UV–vis absorption spectra versus the number (n) of LBL-assembled Nafion/PVI–dmeOs films.

suggest a repeatable and uniform assembly of Nafion films. For the $(\text{Nafion/PVI-dmeOs})_n$/CNT electrodes with '$n$' = halves, the gradual increase of membrane resistance with the growth of LBL-assembled films gradually enhances the inhibition effect on the redox reaction of the newly introduced PVI–dmeOs molecules on the outermost layer, leading to the gradually decreased anodic peak currents.

3.1.2. UV–vis measurements of the LBL-assembled $(\text{Nafion/PVI-dmeOs})_n$ films. LBL assembly of $(\text{Nafion/PVI-dmeOs})_n$ films was examined using UV–vis absorption spectroscopy. An obvious peak at about 287 nm was observed after the quartz was dipped in the solution containing PVI–dmeOs and PEGDGE, indicating a thin PVI–dmeOs hydrogel film was formed on the quartz surface. The UV–vis absorption spectra of $(\text{Nafion/PVI-dmeOs})_n$ films on quartz with different n values are shown in figure 3. The absorbance at 287 nm increases linearly with the growth of the LBL-assembled Nafion/PVI–dmeOs film numbers (inset in figure 3), indicating that the growth of Nafion/PVI–dmeOs films on the substrate is uniform. A uniform growth of films is a characteristic feature of LBL assembly of films. In contrast to a simple dipping, or a simple dropping and evaporating process, LBL assembly of Nafion/PVI–dmeOs films on electrode substrates (such as CNTs) could exactly control the thickness of the Nafion/PVI–dmeOs layer and therefore the performance of the electrodes.

3.1.3. Morphology measurements of $(\text{Nafion/PVI-dmeOs})_n$ film-modified CNTs by SEM. The surface morphologies of $(\text{Nafion/PVI-dmeOs})_n$ film-modified MWCNTs with different values of n were observed by SEM. Figure 4 illustrates the SEM images of high density vertically aligned $(\text{Nafion/PVI-dmeOs})_n$/CNTs with the n value of 0 (figure 4(A)), 0.5 (figure 4(B)), 3 (figure 4(C)) and 9 (figure 4(D)). It can be observed that deposition of PVI–dmeOs on the surface of CNTs did not cause obvious changes to the surface morphology of CNTs (figure 4(B)), indicating that the PVI–dmeOs film was very thin. However, this thin film of PVI–dmeOs significantly increased the hydrophilicity of the surface of CNTs [24]. Thus it may facilitate a uniform assembly of a Nafion film on the surface of PVI–dmeOs/CNTs through electrostatic interactions. The SEM images of $(\text{Nafion/PVI-dmeOs})_3$ film-modified CNTs (figure 4(C)) clearly show that a uniform film is wrapped on the tip as well as the sidewalls of the top part of the high density vertically aligned MWCNTs, but the sidewalls of the stalk of tubes (about 9 μm long) are clearly naked. The absence of $(\text{Nafion/PVI-dmeOs})_n$ films on the tube sidewalls of the stalk part should be due to a high sterical hindrance to the PVI–dmeOs and Nafion molecules from accessing the stalks of the CNTs during the electrodeposition and the LBL assembly processes. The diameter of the bare CNTs used (figure 4(A)) was measured to be at an average of about 88 nm. According to the diameter of $(\text{Nafion/PVI-dmeOs})_3$/CNTs (at an average of about 205 nm) (figure 4(C)) and $(\text{Nafion/PVI-dmeOs})_9$/CNTs (at an average of about 470 nm) (figure 4(D)), the thickness of one Nafion/PVI–dmeOs film was estimated to be about 20 nm.

3.2. The effect of LBL-assembled $(\text{Nafion/PVI-dmeOs})_n$ film on DA-sensing sensitivity at CNTs

DA responses of bare CNTs and CNTs modified with a growing number of Nafion/PVI–dmeOs films were detected by the LSV technique. LSV curves of $(\text{Nafion/PVI-dmeOs})_n$/CNT

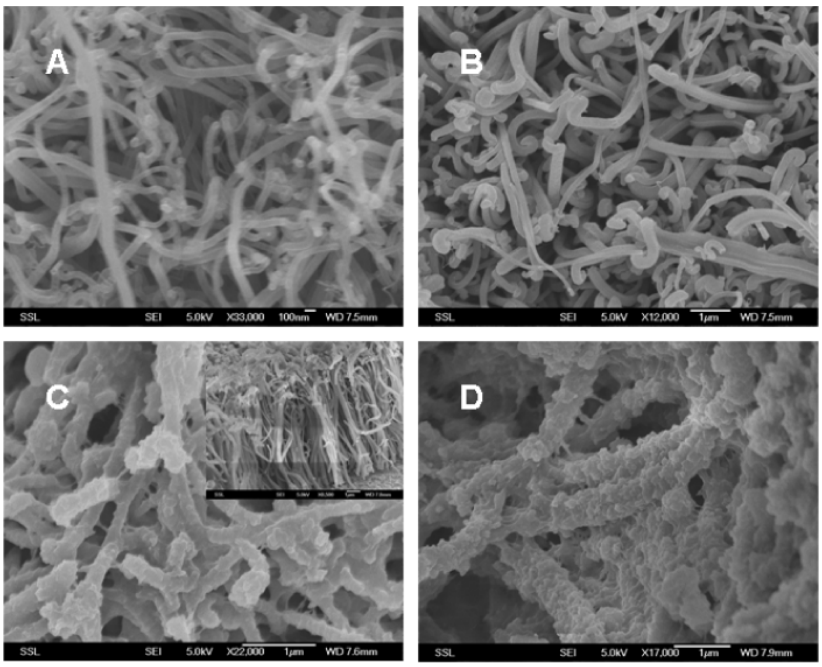

Figure 4. The top view SEM images of high density vertically aligned bare CNTs (A), PVI–dmeOs/CNTs (B), (Nafion/PVI-dmeOs)$_3$/CNTs (C) and (Nafion/PVI-dmeOs)$_9$/CNTs (D). Inset in (C): the side view of post-synthesis cut (Nafion/PVI-dmeOs)$_3$/CNTs.

electrodes with n values of 0, 1, 2 and 3 in PBS containing 10 μM DA are illustrated in figure 5(A) (curve (a), (b), (c) and (d), respectively). Curve (e) is the LSV curve of blank PBS at a (Nafion/PVI-dmeOs)$_2$/CNT electrode, which is used as a representative of (Nafion/PVI-dmeOs)$_n$/CNT electrodes with n = integers. As shown in figure 5(A), the oxidation peak current of DA (at an E_{pa} of about +180 mV) increases obviously with the growth of Nafion/PVI–dmeOs films. The enhancement of DA-detection sensitivity by the LBL-assembled Nafion/PVI–dmeOs films on CNTs could be due to an integrated effect from Nafion layers and PVI–dmeOs layers. Under neutral pH, DA is positively charged, but AA is negatively charged. Nafion, a well-known negatively charged polymer at neutral pH, has been used intensively to coat onto electrodes to enhance DA-detection sensitivity and block the response to AA [14–16]. This effect of Nafion film may be attributed to charge discrimination and accumulation [13]. In addition to Nafion film, the LBL-assembled PVI–dmeOs film may also enhance the DA-detection sensitivity. Similarly to crosslinked redox polymers, the LBL-assembled PVI–dmeOs film becomes insoluble, but may swell in water to form a three-dimensional redox hydrogel. Three-dimensional redox hydrogels are electronically and ionically conductive [20, 21]. Water-soluble and electroactive species like DA and AA can be electrocatalytically oxidized or reduced in the three-dimensional redox hydrogels [14, 23].

Due to a reversible electrochemical redox reaction of PVI–dmeOs, LSVs of a (Nafion/PVI-dmeOs)$_n$/CNT ($n \geqslant 0.5$) electrode in PBS exhibited an oxidation peak at E_{pa} of about +104 mV (as illustrated in curve (e) in figure 5(A)), which is close to the E_{pa} of DA (≈+180 mV). To precisely define and quantify the DA oxidation peak, the LSVs of (Nafion/PVI-dmeOs)$_n$/CNT electrodes in blank PBS were subtracted as backgrounds from their respective LSVs in DA solutions. Background-subtracted LSVs of bare CNTs and the CNTs modified with growing numbers of Nafion/PVI–dmeOs films in PBS containing 10 μM DA are shown in figure 5(B). The background-subtracted LSVs are sharper and better defined than the original LSVs. The derived LSVs clearly show that the DA oxidation peak current in the 10 μM DA solution increase monotonically with the number increase of Nafion/PVI–dmeOs films (n = 0–3). Statistical data of DA oxidation peak current densities read from the derived LSVs in 10 and 50 μM DA solutions for CNTs modified with different numbers of Nafion/PVI–dmeOs films are illustrated in the inset in figure 5(B). Results show that the peak current densities of both DA solutions increase monotonically with the film number increased from 0 to 3, and then diminish when the (Nafion/PVI-dmeOs)$_n$ film grows further. The LSV peak current density of (Nafion/PVI-dmeOs)$_3$/CNT electrodes in response to 10 μM and 50 μM DA solutions was 51.4 ± 9.4 (mean ± SEM) μA cm^{-2} and 119.1 ± 18.0 (mean ± SEM) μA cm^{-2}, respectively, which was about 7.3 and 3.9 times those for bare CNTs (7.0 ± 1.3 and 30.3 ± 7.5 μA cm^{-2}, respectively). The diminishing of the DA oxidation peak currents at high film numbers suggests that the enhancing effect on DA-detection sensitivity caused by the DA accumulation effect of Nafion films and the electrocatalytic effect of PVI–dmeOs films have been counteracted and even surpassed by the inhibiting effect of these films on the conductivity of the composite electrodes.

Owing to their subtle electronic properties, CNTs have been proved to possess strong electrocatalytic activities to DA [7, 9]. This study demonstrated that MWCNTs underlying the (Nafion/PVI-dmeOs)$_n$ films also exhibit strong electrocatalytic activities to DA. A background-subtracted

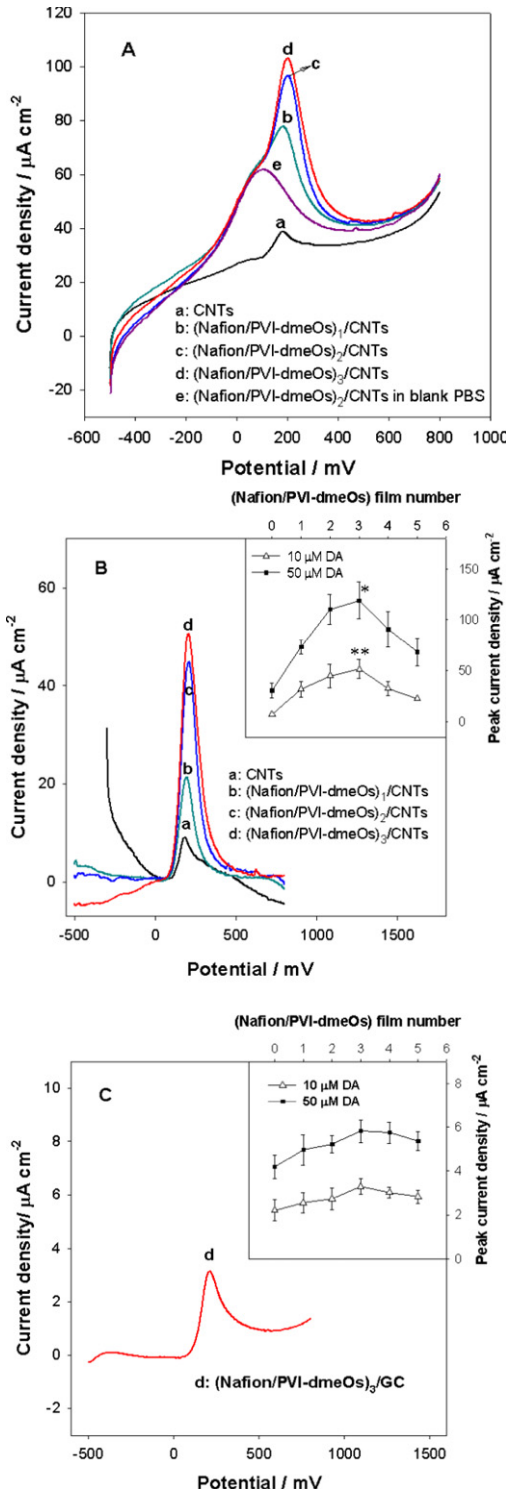

Figure 5. LSVs (A) and background-subtracted LSVs ((B), (C)) in PBS-containing 10 μM DA at CNT ((A), (B)) or GC (C) electrodes without modification (a), or modified with growing $(\text{Nafion/PVI-dmeOs})_n$ films ((b), $n = 1$; (c), $n = 2$; (d), $n = 3$). Curve (e) is the LSV response of blank PBS at the CNT electrode modified with a $(\text{Nafion/PVI-dmeOs})_2$ film. Scan rate: 0.05 V s^{-1}, scan range: -0.5–$+0.8$ V. Inset in (B) and (C): statistical data of peak current densities read from derived LSVs in PBS-containing 10 μM (hollow triangle) and 50 μM (solid square) DA solutions versus the number of Nafion/PVI–dmeOs films on CNT (B) ($n = 5$) and GC (C) ($n = 3$) electrodes. Values marked with * are statistically difference with $p < 0.05$; ** indicates a significant difference with $p < 0.01$ versus bare CNT electrodes (Student's t-test).

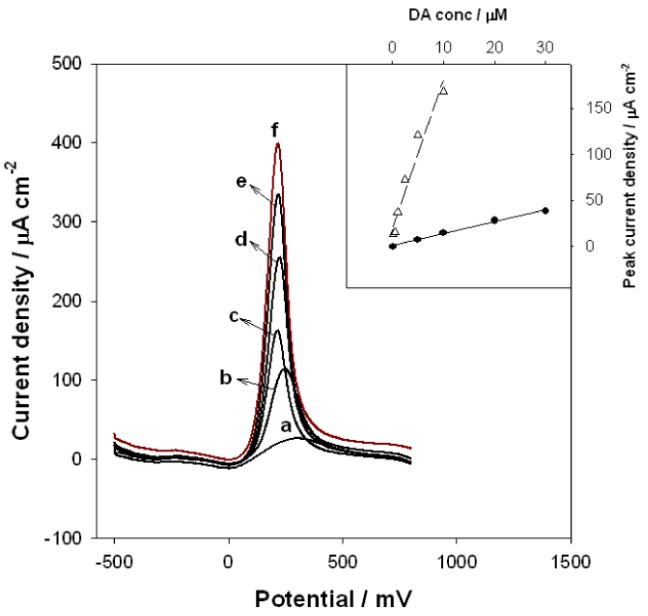

Figure 6. Background-subtracted LSVs of 1 μM (a), 5 μM (b), 10 μM (c), 25 μM (d), 50 μM (e) and 75 μM (f) DA in PBS at a $(\text{Nafion/PVI-dmeOs})_3$/CNT electrode. Scan rate: 0.05 V s^{-1}. Scan range: -0.5–$+0.8$ V. Inset: working curves of peak current densities read from the derived LSVs at the $(\text{Nafion/PVI-dmeOs})_3$/CNT electrode (hollow triangle) or a bare CNT electrode (solid circle) in PBS containing DA versus the DA concentration.

LSV of a $(\text{Nafion/PVI-dmeOs})_3$/GC electrode in PBS containing 10 μM DA (curve (d)) is shown in figure 5(C). Statistical data of peak current densities of background-subtracted LSVs in 10 and 50 μM DA solutions at GC electrodes modified with growing numbers of Nafion/PVI–dmeOs films are illustrated in the inset in figure 5(C). The LSV peak current densities of 10 μM and 50 μM DA solutions at $(\text{Nafion/PVI-dmeOs})_3$/GC electrodes were 3.3 ± 0.3 (mean $\pm$ SEM) and 5.8 ± 0.5 (mean $\pm$ SEM) μA cm^{-2}, respectively, which were only 6.4% and 4.9% of the respective values at $(\text{Nafion/PVI-dmeOs})_3$/CNT electrodes.

The background-subtracted LSVs of a $(\text{Nafion/PVI-dmeOs})_3$/CNT electrode in different concentrations of DA solutions (in PBS) are illustrated in figure 6. The calibration curve of LSV peak current densities versus DA concentration is shown in the inset in figure 6 (hollow triangle). The LOD (signal-to-noise ratio: 3) was determined to be 0.05 μM DA at the $(\text{Nafion/PVI-dmeOs})_3$/CNT electrode. The linear range of the LSV response was 0.1–10 μM DA, with a linear regression coefficient of 0.97, and the DA-detection sensitivity (i.e. the slope of the calibration curve) was 8.15 μA cm^{-2} μM^{-1}. In contrast, at a bare CNT electrode (solid circle in the inset in figure 6), the LOD of DA was 2.5 μM and the DA-detection sensitivity was only 1.24 μA cm^{-2} μM^{-1}. Obviously, assembly of $(\text{Nafion/PVI-dmeOs})_3$ films on MWCNTs greatly enhanced the sensitivity of DA detection, and lowered the LOD of DA. This low level of LOD could allow $(\text{Nafion/PVI-dmeOs})_3$/CNT electrodes to be suitable for direct sensing DA levels in physiological samples, which are normally at the level of 10^{-8}–10^{-7} M [2, 3].

4. Conclusions

After electrodeposition of a thin PVI–dmeOs film on vertically aligned high density MWCNTs, Nafion and PVI–dmeOs films have been successfully LBL-assembled on the surface of PVI–dmeOs/CNT electrodes. In contrast to a simple dipping of CNTs in Nafion solution, or dropping and evaporating of Nafion solution on the surface of CNTs, LBL assembly of Nafion/PVI–dmeOs films on PVI–dmeOs/CNTs could exactly control the thickness of the Nafion/PVI–dmeOs layers and therefore the performance of the as-formed $(\text{Nafion/PVI-dmeOs})_n$/CNT electrodes. LBL assembly of Nafion/PVI–dmeOs films on CNTs significantly enhanced their LSV response sensitivity to DA, with the maximum enhancement at $(\text{Nafion/PVI-dmeOs})_3$ film-modified electrodes. In addition, the CNT electrode substrate underlying the $(\text{Nafion/PVI-dmeOs})_3$ films exhibited strong electrocatalytic activity to DA, therefore further enhancing the DA-detection sensitivity of $(\text{Nafion/PVI-dmeOs})_n$/CNT electrodes. It can be concluded that LBL assembly of $(\text{Nafion/PVI-dmeOs})_3$ films on MWCNT electrodes provides an effective and reproducible way for enhancing the sensitivity of DA sensing. The newly fabricated $(\text{Nafion/PVI-dmeOs})_3$/CNT electrodes may be developed as an ideal biosensor for direct and *in situ* measurement of DA levels in physiological samples.

Acknowledgments

This work was supported by the Academic Research Grant of Talent Introducing Program of Zhengzhou University and the Scientific Research Foundation for the Returned Overseas Chinese Scholars, Ministry of Education of China to HFC.

References

[1] Hirsch E, Graybiel A M and Agid Y A 1988 *Nature* **334** 345–8
[2] Wightman R M, May L J and Michael A C 1988 *Anal. Chem.* **60** 769A–79A
[3] Mo J W and Ogorevc B 2001 *Anal. Chem.* **73** 1196–202
[4] Parsons L H and Justice J B Jr 1992 *J. Neurochem.* **58** 212–8
[5] O'Neill R D 1994 *Analyst* **119** 767–79
[6] Iijima S 1991 *Nature* **354** 56–8
[7] Dresselhaus M S 1992 *Nature* **358** 195–6
[8] Treacy M M J, Ebbesen T W and Gibson J M 1996 *Nature* **381** 678–80
[9] Luo H X, Shi Z J, Li N Q, Gu Z N and Zhuang Q K 2001 *Anal. Chem.* **73** 915–20
[10] Britto P J, Santhanam K S V, Rubio A, Alonso J A and Ajayan P M 1999 *Adv. Mater.* **11** 154–7
[11] Chen R S, Huang W H, Tong H, Wang Z L and Cheng J K 2003 *Anal. Chem.* **75** 6341–5
[12] Poh W C, Loh K P, Zhang W D, Triparthy S, Ye J S and Sheu F S 2004 *Langmuir* **20** 5484–92
[13] Ciszewski A and Milczarek G 1999 *Anal. Chem.* **71** 1055–61
[14] Ju H, Ni J, Gong Y, Chen H and Leech D 1999 *Anal. Lett.* **32** 2951–64
[15] Chou J, Ilgen T J, Gordon S, Ranasinghe A D, McFarland E W, Metiu H and Buratto S K 2009 *J. Electroanal. Chem.* **632** 97–101
[16] Castro S S L, Mortimer R J, de Oliveira M F and Stradiotto N R 2008 *Sensors* **8** 1950–9
[17] Gregg B A and Heller A 1990 *Anal. Chem.* **62** 258–63
[18] Ohara T J, Rajagopalan R and Heller A 1994 *Anal. Chem.* **66** 2451–7
[19] Gregg B A and Heller A 1991 *J. Phys. Chem.* **95** 5970–5
[20] Pickup P G, Kutner W, Leidner D R and Murray R W 1984 *J. Am. Chem. Soc.* **106** 1991–8
[21] Mathias M F and Haas O 1993 *J. Phys. Chem.* **97** 921–5
[22] Doherby A P and Vos J G 1992 *J. Chem. Soc. Faraday Trans.* **88** 2903–7
[23] Doherby A P, Stanley M A and Vos J G 1995 *Analyst* **120** 2371–6
[24] Cui H F, Ye J S, Zhang W D and Sheu F S 2009 *Biosens. Bioelectron.* **24** 1723–9
[25] Zhang W D, Wen Y, Lin S M, Tjiu W C, Xu G Q and Gan L M 2002 *Carbon* **40** 1981–9
[26] Zhang W D, Wen Y, Tjiu W C, Xu G Q and Gan L M 2002 *Appl. Phys.* A **74** 419–22
[27] Ye J S, Wen Y, Zhang W D, Gan L M, Xu G Q and Sheu F S 2003 *Electroanalysis* **15** 1693–8
[28] Cui H F, Ye J S, Zhang W D, Wang J and Sheu F S 2005 *J. Electroanal. Chem.* **577** 295–302
[29] Wang J, Musameh M and Lin Y H 2003 *J. Am. Chem. Soc.* **125** 2408–9